Life-cycle energy and carbon saving potential of Wire Arc Additive Manufacturing for the repair of mold inserts

Life-cycle energy and carbon saving potential of Wire Arc Additive Manufacturing for the repair of mold inserts

Paolo C. Priarone [a,*], Gianni Campatelli [b], Angioletta R. Catalano [a], Francesco Baffa [b]

[a] Politecnico di Torino, Department of Management and Production Engineering, Corso Duca degli Abruzzi 24, 10129 Torino, Italy

[b] Università degli Studi di Firenze, Department of Industrial Engineering, Via di S. Marta 3, 50139 Firenze, Italy

* Corresponding author (P.C. Priarone)
Email: paoloclaudio.priarone@polito.it
Ph.: (+39) 011 0907259
Fax: (+39) 011 0907299
ORCID: 0000-0003-4226-7697

Abstract

Additive Manufacturing (AM) has been identified as a disruptive technology, that enables the transition to Industry 4.0 and allows companies to re-think and re-design both their products and manufacturing approaches. In such a context, the opportunity of using AM to extend the life of a product through repair could also allow the founding principles of the circular economy to be implemented. This paper deals with the development of a repair procedure for mold inserts, made of H13 steel, that are used to cast aluminum cylinder heads for internal combustion engines. The repair operations were experimentally performed in a hybrid additive-subtractive manufacturing center used for Wire Arc Additive Manufacturing. Once the technological and quality results that are required by the strict industrial standards had been verified, the life-cycle energy and carbon footprint of the repair approach were quantified and compared with those of the conventional substitution-based approach. Overall, at the end of the first life of the insert, the results highlighted that the WAAM- and repair-based approach could allow potential savings for both performance metrics, compared with the insert being machined from a massive workpiece as a substitute, despite requiring several manufacturing steps and incoming feedstock material characterized by a high embodied energy. Moreover, the environmental benefits of the proposed approach are amplified when multiple repair loops are considered, even for a lower lifespan for the repaired mold insert.

Keywords: Sustainable manufacturing; Wire arc additive manufacturing; Repair; Comparative life-cycle assessment; Steel mold insert

1. Introduction

In recent decades, the massive consumption of natural resources, related to industrial developments, has led to considerable environmental, economic and social impacts. The manufacturing sector contributes to the harmful effects on the environment through material wastage, the consumption of resources and energy, and the emissions of CO_2 and other greenhouse gases (GHG) associated with climate change. The manufacturing and construction sectors are known to play a relevant role in emitting a high percentage of GHGs (24% in 2016, according to data provided by IEA in 2018), either directly through the use of fossil fuels, or by consuming energy and resources during the support operations (Sutherland et al., 2008). Therefore, several research studies have focused on the optimization of energy and resource efficiency, from the single unit-process up to the entire manufacturing company. In addition, since the increasing pace of waste production, coupled with the upstream consumption of materials, has led to the current concern about the rapid turnover of products, an overall solution could be the rethinking of the End-of-Life (EoL) concept and of waste, that is, extending the life of products by returning value to them (Ashby, 2016). After the use phase, different technological strategies can be adopted to postpone the disposal of the so-called 'EoL products' and thus to extend their life, thereby allowing EoL products to re-enter a lifecycle and effectively close the loop (King et al., 2006). Industrial systems, which are restorative and regenerative by nature and design, follow the Circular Economy principles (Ellen MacArthur Foundation, 2013), thereby overcoming the limitations of the linear approach underlying the take-make-dispose principle that has resulted in an inadequate and unsustainable situation of imminent material depletion (Jawahir and Bradley, 2016).

1.1 Additive manufacturing and sustainable development

In this context, Additive Manufacturing (AM) is one those advanced manufacturing technologies that allow companies to re-think how to manufacture products (Despeisse et al., 2017). Different industrial and academic research efforts have recently started to be structurally dedicated to understanding the (intended or unintended) consequences of the adoption of AM and its impact on sustainable development (such as those of Colorado et al., 2020; Dilberoglu et al., 2017; Machado et al., 2019; Khorram Niaki et al., 2019a). The environmental impact of AM is still a matter of discussion (Liu et al., 2018), because of the many factors that can influence quantitative evaluations, which are mainly focused on energy efficiency at the machine level, and sometimes highlight a higher specific energy consumption of AM than conventional manufacturing approaches (Sauerwein et al., 2019). However, the different benefits of AM, in terms of material, energy, and cost efficiency, should be evaluated and recognized across the whole life cycle of a product (Despeisse et al., 2017; Ford et al., 2015). Ford and Despeisse (2016) identified the four main areas in which resource efficiency can be achieved by means of the implementation of AM, namely (*i*) the design of both the product and process, (*ii*) the processing of the input material, (*iii*) make-to-order manufacturing, and (*iv*) closing the loops and re-entering the life cycle. The unique characteristics of AM processes are related to its additive and digital nature. These distinctive peculiarities lead to remarkable transformations in manufacturing systems (Despeisse et al., 2017) and in the paradigm (Chen et al., 2015). AM mimics biological processes in its creation of products by depositing material additively (Ford and Despeisse, 2016), unlike conventional manufacturing processes in which the mass is conserved and deformed or removed from an initial block of material. Material deposition in an additive layer-wise manner allows complex designs to be embedded at the (*i*) micro-scale, via the creation of functionally graded materials and in-situ alloying (Rosen, 2014; Srinivas and Babu, 2017), (*ii*) meso-scale, with the possibility of realizing regular lattice structures and foams (Rosen, 2014), and (*iii*) macro-scale, by fabricating geometric features that would otherwise not be achievable by means of conventional processes. This capability, which is known as 'complexity-for-free' (Khorram Niami et al., 2019b), enables load-adapted and/or nature-inspired (re)designed components to be optimized and made lighter (Emmelmann et al., 2011; Huang et al., 2015), even in combination with other conventional processes (Bambach et al., 2017). This results in an unprecedented resource efficiency and reduced waste generation, and it leads not only to a reduction in energy consumption during the use phase (Ford et al., 2015), but also in the manufacturing phase, via a reduction in material yields. Such a reduction translates into lower impacts of the material-related energy demand on (*i*) non-value material processing and (*ii*) recycling in the EoL stage (Chen et al., 2015; Ford et al., 2015). The additive nature of AM processes also leads to part consolidation in more efficient and simpler assemblies (Despeisse and Ford, 2015; Klahn et al., 2014). Moreover, the use of a single material in the manufacturing of all the sub-parts of an assembly leads to (*i*) dematerialization, (*ii*) a reduction in the inventory and storage sites, (*iii*) the simplification of assembly lines (Sauerwein et al., 2019) and (*iv*) modifications of the supply chains (Despeisse et al., 2015). In fact, AM techniques do not require any specialized tools, fixtures or molds (Mani et al., 2014; Khorram Niaki et al., 2019a), and its digital nature introduces the possibility of creating on-demand parts (new or spare ones) (Sauerwein et al., 2019). Centralized mass production is gradually being substituted by decentralized manufacturing, in which over-production and transportation are reduced (Liu et al., 2018; Sauerwein et al., 2019) as a result of the evolution of AM in Direct Digital

Manufacturing (DDM), which relies on an interconnection between additive manufacturing equipment, computers and software, by means of a network (Chen et al., 2015). In such a manufacturing paradigm, a new interaction takes place among the stakeholders, and the consumer becomes a prosumer (Cruz Sanchez et al., 2020; Khorram Niaki et al., 2019b), since he/she has the possibility of customizing products by actively participating in defining the product requirements. The end-user can optimize the time consumption, since it is possible to easily intervene in digital design CAD models (Wits et al., 2016). Such an interaction allows new and more service-based business models and sustainability interests to be aligned (Ford et al., 2015). This interaction also facilitates the decoupling of the environmental impacts, attributable to both manufacturing and consumption, from the generated social and the economic value. Such a process transforms residues, wastes and obsolete products into valuable assets within a circular value ecosystem (CVES) (Ford et al., 2015; Scheel et al., 2020).

1.2 AM for remanufacturing, refurbishment and repair

AM has also been recognized as an enabler of circular design strategies, due to the opportunities of extending the lifespan of a product (Sauerwein et al., 2019). AM can be employed not only for the production of new high-value customized end-use products in small batches (Despeisse et al., 2017), but also to (*i*) improve their durability through optimization by means of a redesign, and/or (*ii*) upgrade or repair and remanufacture damaged products, either *in-situ* or through the production of spare parts on demand (Ford et al., 2015; Sauerwein et al., 2019). Remanufacturing, refurbishment and repairing are restorative processes that change damaged parts into a workable condition in order to return value to a product (Leino et al., 2016). In the manufacturing context, these activities play a strategic role in the scope of the circular economy because these products, components and materials are aimed at maintaining the utility and value of a product throughout its entire lifetime (Saboori et al., 2019). Repairing and remanufacturing, by means of AM, take on particular importance for complex and high-value components, whose replacement would be expensive in terms of both cost and time (Kaierle et al., 2017). These restorative activities are increasingly being adopted in the automotive, household appliance, industrial machinery, aerospace, marine and power generation fields. An overview of the main industrial applications, together with their advantages and disadvantages, is given in this Section. Moreover, Section 1.3 focuses on the currently-exploited technologies, which deserve a more detailed digression. Wasono et al. (2019) provided a literature review on recent applications of AM for repair and restoration in different industrial sectors, highlighting that the most frequently investigated components are turbine blades and impellers. In fact, Liu et al. (2014) demonstrated the feasibility of using Laser Engineered Net Shaping (LENS) to repair casting defects in turbine components made of Inconel 718 and Waspaloy. Zhang et al. (2018) exploited a laser-aided Direct Metal Deposition (DMD) process to deposit a titanium-based alloy and to validate the automated modelling of the worn surface of an engine blade. Bi and Gasser (2011) studied the tool-path generation for repairing nickel-based blades by means of Laser-based Direct Metal Deposition, while proposing an automated modelling of the damaged surfaces, similarly to Qi et al. (2010). Petrat et al. (2016) investigated a powder-based DED process for a near-net-shape repair of a gas turbine burner made of Inconel 718, by varying different parameters and showing the capabilities of laser metal deposition. Also, the repair of engine components and transmission gearboxes (Yin et al., 2018), new rails (Lewis et al., 2015), and valve actuators from the marine sector (Widener et al., 2016) has been explored. The latest technological advances have led to the remanufacturing of molds and dies to also be considered feasible, although they had previously been limited to traditional welding techniques (Morrow et al., 2007) for fixing objects damaged by, for example, surface corrosion and cracking due to the cyclic thermo-mechanical loadings they have to undergo during their lifetime (Bennett et al., 2019). In the last few decades, it has frequently been reported that when several high-performance components, such as turbine blades or molds and dies are damaged, they are scrapped and recycled without preserving their geometries or their associated value. Even though recycling through melting offers the possibility of recovering material with a smaller necessary amount of energy than for material extraction from ores, it is still more energy-intensive than reusing without resorting to melting (Allwood and Cullen, 2011; Saboori et al., 2019), and without reducing a used product to simply embed the value of its raw materials (Ijomah et al., 2007). Remanufacturing, reconditioning and repairing are the most frequently indicated choices since they can fully recover the value of the resources employed to manufacture a product, thereby reducing the need for further new resources (Sutherland et al., 2008). They lead to the possibility of recovering between 20% and 80% of the production costs, compared to conventional manufacturing routes (Zhu et al., 2004), thus reflecting on the cost of the final product cost (Chen et al., 2014). Furthermore, when the cost for remanufacturing a product is equal to that of purchasing one, a considerable time saving can be achieved, above all for those components that require months for their new production (Liu et al., 2017). Moreover, when 100% of the lifetime is recovered in a repaired or remanufactured product, emergencies for unplanned repairs and downtimes are avoided (Bennett et al., 2019) as well as related increases in costs (Chen et al., 2014). Although the benefits of remanufacturing are highly sensitive to different factors (Sutherland et al., 2008), and considering its own environmental impacts due to transportation, cleaning operations, the consumption of resources during testing processes, as well as the recycling of non-reusable materials (Zhang et al., 2020), remanufacturing is known to introduce substantial overall savings. Moreover, over half of the total energy and labor required for new production can be saved, and lower CO_2 emissions occur, even though they are dependent on the amount of material needed for the repairs (Wilson et al., 2014). Although additive manufacturing techniques can require a higher energy consumption during repair operations than conventional methods (Walachowicz et al., 2017), the advantages, apart from improving material use efficiency, should be evaluated across the whole life cycle, such as, for example, the advantage on the impact of the reduced life-cycle due to the recycling of scrap material (Bennett et al., 2019).

1.3 WAAM processes for repair

Repair operations can be employed, for both geometric and structural restoration, by fixing sub-surface defects (Liu et al., 2017). In order to evaluate the best candidate for a repairing operation, it is necessary to analyze the three main steps needed to perform such an operation on a high-value component, such as a die or a turbine blade. These steps include:

- *Preparation:* the worn or flawed surfaces are machined to obtain a known shape on the surface;
- *Deposition:* a filler material is deposed onto the prepared surface;
- *Finishing:* the final shape of the component is achieved through a further machining step, which is required to meet the demanding standards currently in force for high-value components.

A variety of different technologies may be used for the second step. Traditionally, most repairing operations were done via Gas Tungsten Arc Welding (GTAW), which allows a good control of the deposition parameters to be achieved, since the heat input and material feed are decoupled, and it is often used as a reference for comparative quality evaluations pertaining to repair (Ramalho et al., 2011; Yushchenko et al., 2004). Other techniques are characterized by a high complexity and high costs, and in certain cases they require extensive secondary machining or are even manually driven. Saboori et al. (2019) provided a comprehensive comparison of different techniques used to repair and remanufacture components, including Plasma Transferred Arc (PTA) welding, Electron Beam (EB) welding, High-Velocity OxyFuel (HVOF) thermal spraying, and Electro Spark, together with AM laser-based Direct Energy Deposition (DED) processes (Saboori et al., 2019). Other authors have contributed to the literature while focusing on repair activities via AM, especially for metal components. This literature provides overviews from the object design and systems perspectives (Rahito et al., 2019), and focuses on specific application fields and case studies, such as dies and molds (Chen et al., 2014), or from the viewpoint of a specific AM technology, e.g., DED (Saboori et al., 2019) or Cold Spraying (CS) (Li et al., 2018). According to the literature, DED and CS are the most suitable AM technologies for repair and remanufacturing applications (Leino et al., 2016; Rahito et al., 2019). These processes are in fact particularly interesting for the support of the repairs of metal components since they allow a new layer of material to be added to an existing geometry. The same approach is generally not feasible when powder-bed-based solutions are used, where it is mandatory to create a part starting from a base plate with a flat surface. Nonetheless, Electron Beam Melting (EBM) has been employed to deposit both similar materials (Mandil et al., 2016) and dissimilar ones (Hinojos et al., 2016) for improvement or restorative purposes. DED processes may be based on laser, electron beam or an electrical arc, as they have the aim of melting a feedstock in the form of metal powder or solid wire. The use of powder generally allows a better accuracy to be achieved at a lower deposition rate, while the use of wire allows a faster but less accurate process to be obtained (Cunningham et al., 2018). One of the emerging technologies used to automate and increase the productivity of repair operations is Wire Arc Additive Manufacturing (WAAM), which is basically a 3D welding process in which a geometrical feature is created using a layer-by-layer approach or a surface is clad by creating a continuous layer on a free-form surface. The main advantages of WAAM are the possibility of creating large parts, up to some meters (Bandari et al., 2015), at a very high deposition rate, which could reach a higher value than 10 kg per hour using such materials as steel, aluminum, titanium and others (Williams et al., 2016). The main drawback of WAAM is that the created surfaces are characterized by a high degree of waviness, and machining operations are mandatory, after the deposition step, to achieve the required surface finish. This is not an issue for repair operations, since machining is always required however to recreate the worn functional surfaces. WAAM also allows such a technology to be easily integrated with existing processes and machines, thus creating a hybrid additive-subtractive process that could dramatically increase the productivity of a repair process, thanks to a reduction in the change-over times and to the enabling of a streamline approach to repair complex parts (Pragana et al., 2021). Moreover, such an innovative repair technique leverages on both processes (i.e., additive and subtractive), and overcomes the limits of each one, such as the poor surface finishing associated with AM or the impossibility of realizing highly complex features in conventional machining operations (Peng et al., 2017; Zheng et al., 2020, Bennett et al., 2019). Many technologies may be used to implement WAAM, for example, GMAW (Gas Metal Arc Welding), GTAW and PAW (Plasma Arc Welding). In GMAW, an electric arc is created between the tip of a consumable electrode (wire) and the part that has to be repaired, albeit under the protection of inert shielding gas, while the electrode in GTAW and PAW, which is usually made of tungsten, is not consumable, and the material is supplied though a lateral feeding unit (Wang et al., 2021). GMAW is the most frequently used deposition technology, since it is the most flexible; in fact, the wire feedstock for this variant of the WAAM technology is coaxial to the torch, and the fusion rate is higher, since the filler material for GTAW and PAW is not melted directly by the arc, but is fed to the molten pool, which is at a lower temperature. Further increases in the deposition rate could be achieved by using a double wire feeding system that would also allow functionally graded materials to be created by varying the relative WFS (Wire Feed Speed) of the two systems (Wang et al., 2019). The main drawback in using GMAW is the high heat input of the welding process, which may lead to distortion, excessive remelting of the substrate or lower layers and metallurgical alterations of the microstructure of the material. Welding source manufacturers have developed several approaches to reduce the heat input, such as the modulation of the pulse that ignites the arc or the introduction of an alternative micromovement of the wire that promotes an easier and colder detachment of a molten metal drop from the wire, as in the CMT (Cold Metal Transfer) approach, which was patented by Fronius. Such an expedient leads to a reduction in the dilution, which may arrive at 3% for CMT and 28% for the traditional GMAW approach (Martina et al., 2019), thereby supporting the preservation of the original base metal properties and saving material during the buildup of the repair layer.

1.4 Aim and structure of the paper

Overall, the literature highlights the potential benefits of Additive Manufacturing and product repair for the implementation of the principles of sustainable development and a circular economy. However, the literature lacks information about the quantification of the cradle-to-grave environmental benefits of repair-based manufacturing approaches. Only a few analyses are based on Life Cycle Assessment (LCA). For instance, Liu et al. (2013) investigated the energy consumption and environmental emissions during the entire life cycle of a diesel engine, by comparing the originally-manufactured part to the re-manufactured counterpart, while identifying the most demanding phase of product's life. Similarly, Wilson et al. (2014) compared the impact of manufacturing or re-manufacturing a component via laser direct deposition. Peng et al. (2017) assessed a laser cladding process while comparing the environmental effects of different manufacturing routes, such as conventional manufacturing and additive manufacturing, in the case of an impeller production. Bennett et al. (2019), instead, evaluated the results of traditional repairing processes and DED ones for aluminum four-cylinder engines, during their whole life cycle. The present paper focuses on the development of a repair procedure for a mold insert made of H13 steel and is aimed at quantifying the life-cycle energy and carbon footprint savings that can be obtained when both cradle-to-grave boundaries and multiple repair loops are considered. The experimental setup of the hybrid additive-subtractive machine, as well as a description of the case study and the applied repair procedure are presented in Section 2, together with a part quality assessment. Section 3 details the comparative life-cycle energy and carbon footprint assessment methodology, the results of which are discussed in Section 4. Finally, the main conclusions and research outlooks are summarized in Section 5.

2. Materials and methods

The deposition source used for the repair operations was a TPSi 320 CMT, manufactured by Fronius (Figure 1*a*), which was selected since it allows material to be deposited with a low heat input and high deposition rate, by means of the CMT process. This system couples together a pulsed electrical arc with a high-frequency and alternated micromovement of the welding wire, thus facilitating the detachment of a molten metal drop from the wire. The welding source was installed on a machining center, i.e., a DMU 75 Monoblock by DMG Mori (Figure 1*b*), in order to create a hybrid additive-subtractive production center capable of carrying out all the steps required for repairs without the need to move or reposition the metal part. In fact, the surface preparation, deposition and finishing were carried out with the same fixturing on a single machine, thus enabling a streamlined process to be achieved. This hybrid solution was developed within the framework of the RetroFix project (see the 'Acknowledgments' section), and the machine was equipped with a specially-designed torch holder, which could be stored in the automatic tool changer (ATC, in Figure 1*c*), and a ground table for 5-axis operations. This makes it possible to switch from material removal (Figure 1*d*) to layer-wise deposition - and vice versa - in just a few seconds, by starting a special M-function on the NC of the machining center. Therefore, 5-axis deposition and milling toolpaths, both of which are required to repair complex and high value components (such as automotive dies and molds or parts for the energy and aerospace sectors), are implementable. The choice of using a machining center as a base for the hybrid machine, instead of a robot, was expected to lead to a high productivity in the preparation of the surface that has to be repaired, and to obtain a high surface finish and dimensional accuracy at the end of the process, thanks to the high stiffness of the machine and the high precision of the axis movements, even when machining difficult-to-cut materials (such as tool steels, nickel-based alloys, titanium alloys, et cetera).

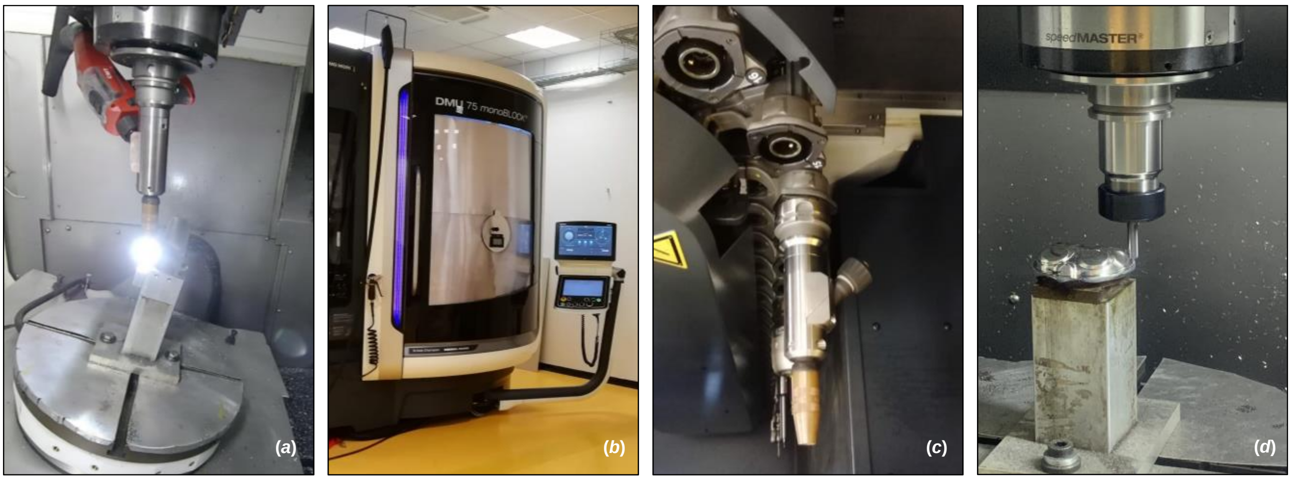

Figure 1. Experimental setup: deposition system (*a*), machining center (*b*), torch holder stored in the ATC (*c*), and milling head (*d*).

2.1. Case study

An insert of a mold used to cast aluminum cylinder heads for internal combustion engines was identified as the case study for this research. A three-dimensional sketch and its overall dimensions are shown in Figure 2*a* and Figure 2*b*, respectively. The insert was made of AISI H13, a hot-work tool steel, belonging to the chromium steel series, that is characterized by a good resistance and hardness at high temperatures. However, one of the main issues of this material is its susceptibility to cracking. For this reason, the number of studies focused on additive manufacturing applications using H13 has recently been increasing. Rajeev et al. (2017) used CMT for deposition and found that the risk of cracking could be reduced by pre-heating the part. Legesse et al. (2018) found a similar result when using a pre-heating system for the production of a brand-new H13 die using a hybrid CMT-based approach. Ge et al. (2019) demonstrated that the deposition of an H13 free-crack block with limited porosity and proper mechanical properties using CMT was also possible. A mold insert is subjected to wear, which is mainly caused by repeated thermal cycles, chemical attack of the aluminum and the subsequent cleanings the tool has to undergo during its service life. As a result, such a mold has to maintain very narrow dimensional tolerances, and the insert should therefore either be substituted or repaired periodically.

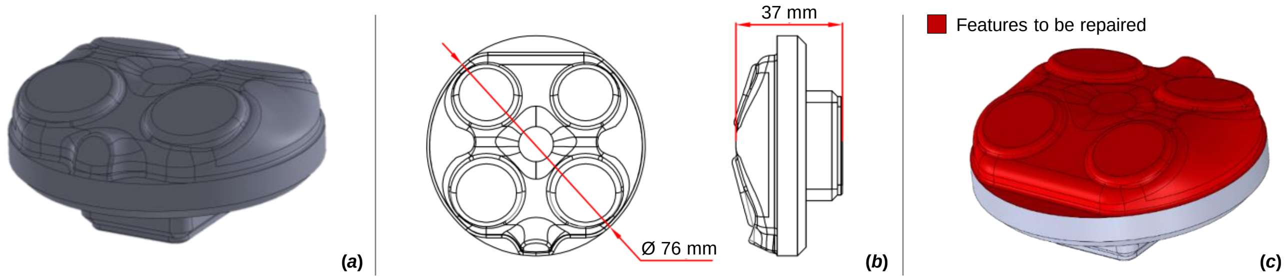

Figure 2. Case study: 3D sketch (*a*), overall dimensions (*b*), and details of the features that have to be repaired (*c*).

Figure 3. Result of the substrate preparation phase (*right*) with reference to the original geometry of the insert (*left*).

2.2. Manufacturing route for repair

A machining-deposition-machining sequence was planned to repair the part. The first step was the removal of the worn material from the top surface of the insert (Figure 2*c*), in order to achieve a crack-free substrate and define a geometrically-known geometry for the subsequent material deposition. During this phase, the creation of a smoother surface resulted to be a more effective manufacturing solution than removing a layer of material of equal thickness. In fact, initial tests highlighted that the presence of small corner radii and vertical surfaces could lead to a lack of filling in the hard-to-reach areas of the features that had to be repaired, even when adopting 5-axis deposition strategies. The geometry defined for the surface preparation had to comply with the competing requirements of (*i*) removing enough material to expose the unworn substrate, (*ii*) avoiding an excessive removal of the material (that should not have exceeded the thickness of the deposited layer), and (*iii*) avoiding sharp corners and abrupt discontinuities of the surface curvature. The result of the substrate preparation phase is shown in Figure 3, in which the machined part (before the deposition phase) is compared with the brand-new insert.

Table 1. Process parameters for H13 deposition.

Parameter	Value
Transfer mode	CMT (Cold Metal Transfer)
Wire feed speed (m/min)	5
Deposition speed (mm/min)	360
Stick-out distance (mm)	14
Shielding gas	98% Argon + 2% CO_2 (with a 15 l/min flux)
Arc correction	-3.0
Dynamic correction	-2.5

The material deposition was carried out by means of the WAAM process. The feedstock material was a 1.0-mm diameter H13 wire, manufactured by Boehler-Uddeholm (with the following chemical composition: Carbon, C = 0.39%; Chromium, Cr = 5.3%; Molybdenum, Mo = 1.3%; Vanadium, V = 0.9%; Manganese, Mn = 0.4%; Silicon, Si = 1.0%; Iron, Fe = balance). The main deposition process parameters are listed in Table 1. The toolpath adopted for the deposition was the result of preliminary tests on the deposition strategy, step-over and the torch orientation. A constant step-over of 3.6 mm was selected, according to the best step-over-to-bead width ratio of 0.738, as fixed by Ding et al. (2015), while the torch was held normal to the deposition surface, as shown in Figure 4*a*. The result of the deposition phase was a continuous layer with no observable lack of material or inclusions (Figure 4*b*). The part was pre-heated at 300°C, and the post-WAAM cooling was performed in an insulated environment, i.e., a bin filled with vermiculite. After the deposition of the H13 layer, the part was milled by adopting the same rough- and (semi-)finish machining parameters used for the production of the brand-new insert, as detailed in Section 3. In order to acquire experimental data to evaluate the environmental impact of the proposed repairing process, all the manufacturing steps were monitored for both the materials (e.g., welding wire, shielding gas) and energy consumption. The deposition step data were measured by an internal logger housed in the welding unit that was able to measure the energy, welding wire and gas consumption of each deposited bead. A logger was created for the machining step, using a National Instrument DAQ device (NI-9215) equipped with current and voltage sensors. Three gauges, produced by LEM (LEM AT 10 B420L, hall effect sensor with open core and a range 0-10A), were used to acquire the current.

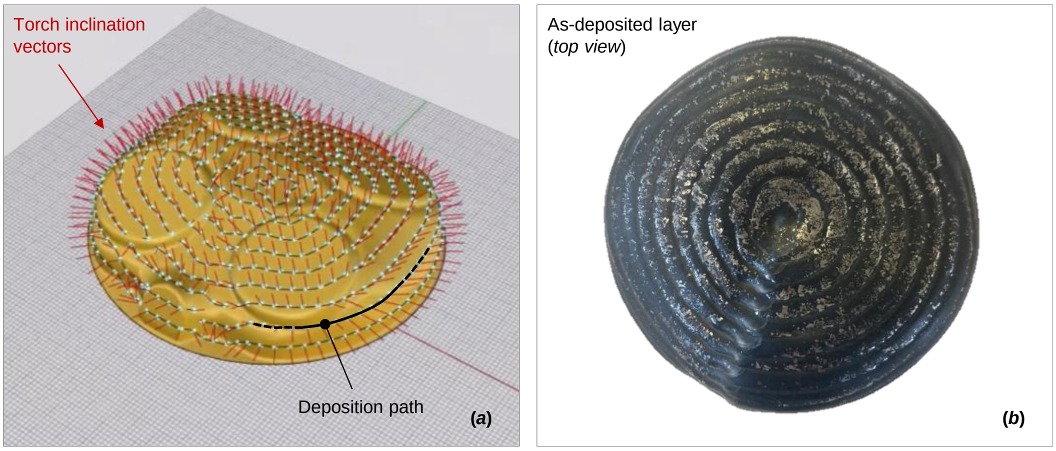

Figure 4. Deposition of the H13 material by means of CMT: deposition path (*a*) and as-deposited layer (*b*).

Moreover, in order to assess the feasibility of the proposed approach, macroscopic and microscopic observations of the produced samples were carried out to verify the thickness of the deposited layer and its metallurgical characteristics. The samples were obtained by sawing the repaired parts along different planes and lapping the cross-sectional surfaces using (*i*) abrasive papers with a progressively decreasing grain size till a 1200 mesh was reached, and (*ii*) diamond powder for the final step. The lapped samples were chemically etched with a 2% NiTal solution, and then analyzed using a metallographic microscope with a magnification ratio of 250x. Figure 5*a* shows the continuity of the repaired layer and its nearly constant thickness, which has a mean value of 2.6 mm on the top surface and 1.5 mm on the lateral surface. The microstructural analysis (Figure 5*b* and Figure 5*c*) highlights the presence of martensite needles, which are characterized by a higher degree of hardness than the substrate. This experimental evidence suggests the need for a heat treatment before the use of the insert. However, despite the requirement of a heat treatment, the analyses ensured that the here adopted repair approach could be adopted to substitute the traditional manual GTAW-based repairing approach.

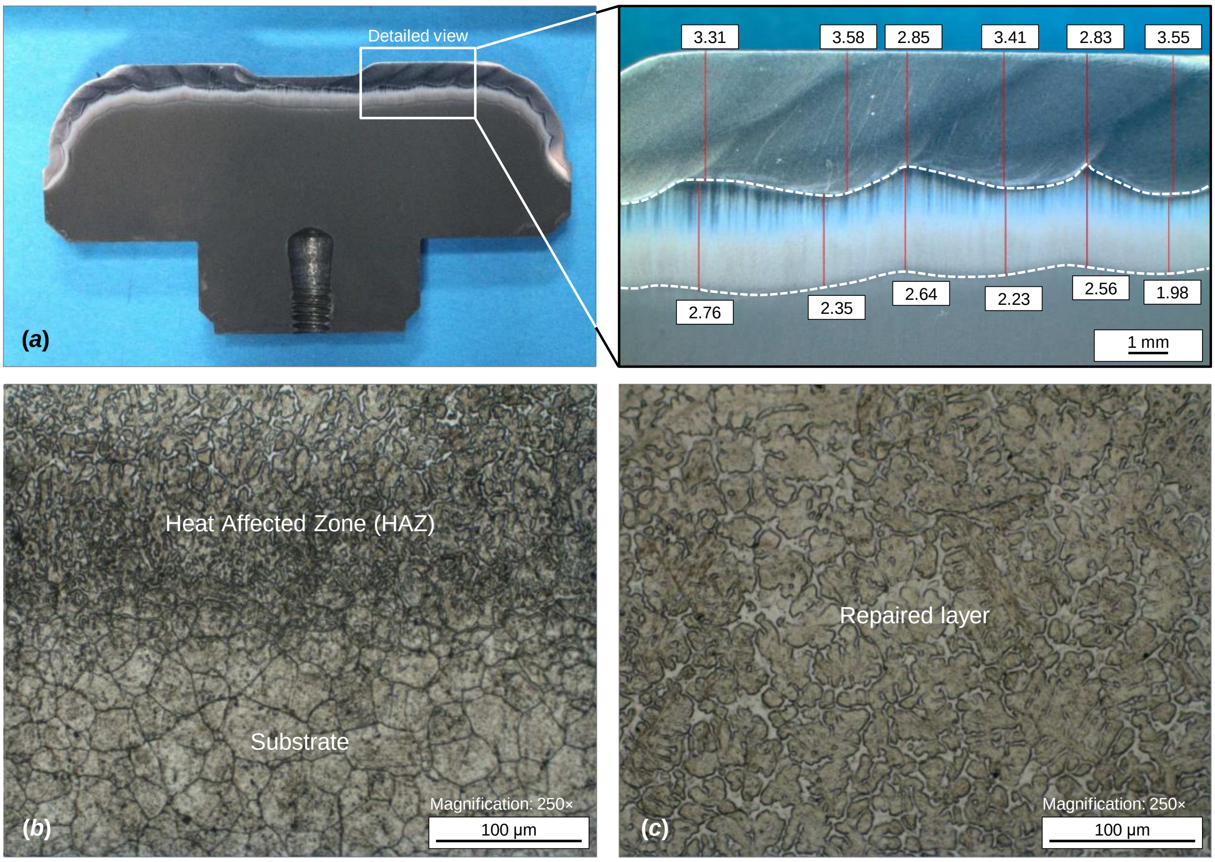

Figure 5. Test case after the repair process: layer thickness (*a*); HAZ microstructures (*b*) and repaired layer (*c*). Courtesy of Aurrenak S. Coop.

3. Comparative life-cycle energy and carbon footprint

Having verified the technological feasibility of the repair approach for the mold insert made of H13 tool steel, the research was then aimed at quantifying the environmental impact of the WAAM-based repair process within the life cycle of the product. The replacement of a worn mold with a brand new one was considered as a benchmark for the assessment. The unit processes and the main flows that are schematized in Figure 6 were considered as the boundaries of the analysis. The Cumulative Energy Demand, CED (also defined as primary energy consumption), and the carbon dioxide equivalent emissions were the selected metrics. Thus, the so-called 'one resource, one emission' approach proposed in Ashby (2013) was followed. This choice is consistent with other research studies aimed at comparing WAAM-based and machining-based manufacturing approaches (Priarone et al., 2019 and 2020; Campatelli et al., 2020). The life-cycle impacts were based on the primary energy of the input material feedstock, the process electricity and resource consumption, as well as the benefits due to recycling. The impacts due to the use phase of the mold insert were excluded from the boundaries of the analysis since the use phase performance was expected to be equal for both scenarios. Moreover, all the ancillary material inputs that are amortized after the production of multiple print jobs were excluded from this study, as it was expected that these inputs would provide negligible contributions to the impact on the cradle-to-grave life cycle. Other product system components that are amortized over their respective lifespans, such as the hybrid additive-subtractive machine and its equipment, and the manufacturing facility infrastructure, were also excluded from this LCA (London et al., 2020).

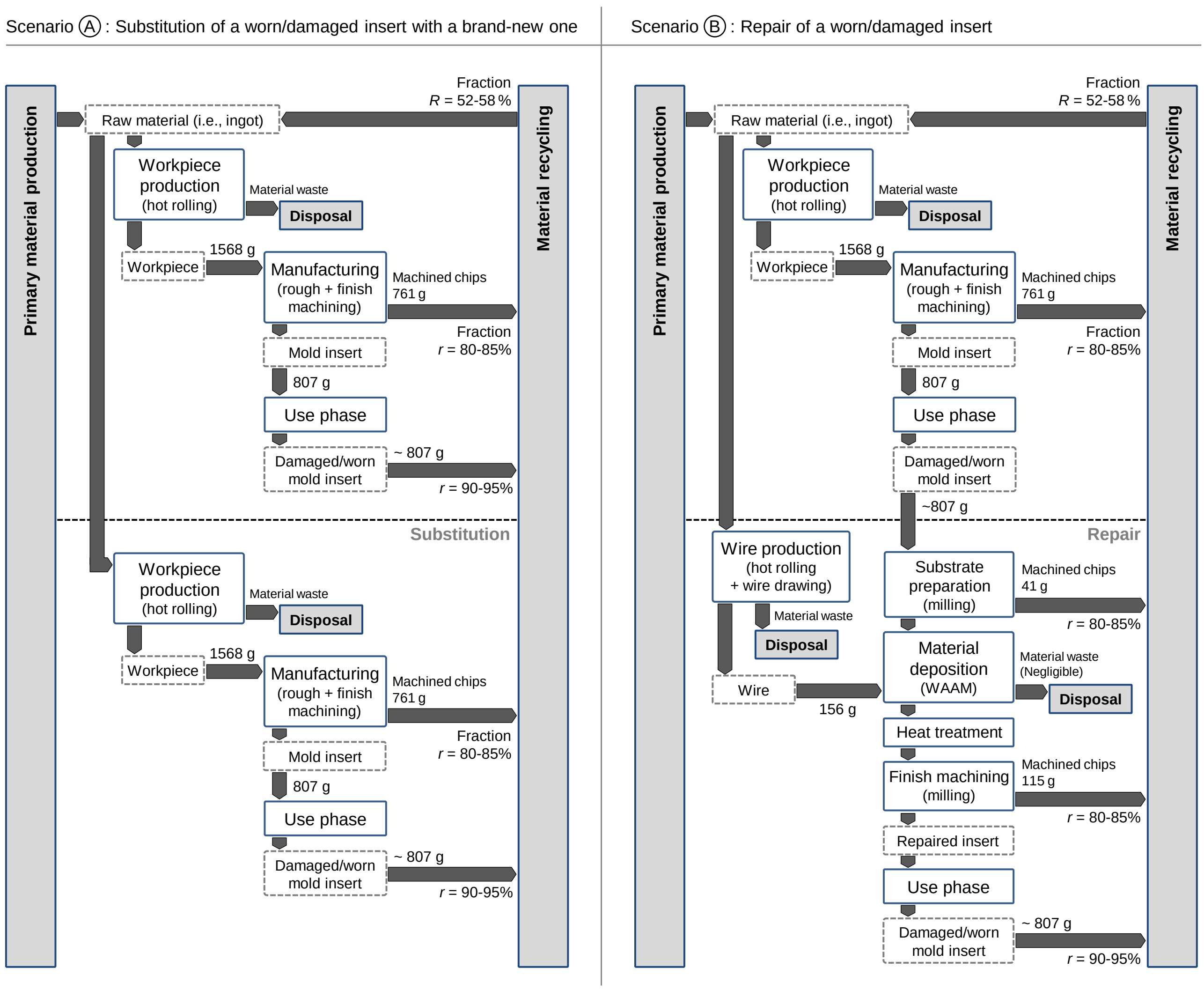

Figure 6. Boundaries of the study for Scenario A (*left*) and Scenario B (*right*).

Different approaches may be applied for the Cumulative Energy Demand indicator. Therefore, substantially different results may be achieved, even when using the same physical energy unit of MJ and targeting the same primary energy use (Frischknecht et al., 2015). Differences arise among the approaches that rely on energy values, when quantifying the CED of fossil-based energy resources, whenever lower or higher heating values are considered, and the energy values adopted for the cumulative energy demand for nuclear and renewable energy sources also differ from each other. Moreover, a further source of discrepancy between the results could be due to the weighting method chosen to aggregate the energies derived from both renewable and non-renewable sources. For the sake of transparency, this research has assumed the best estimates for the incoming feedstock material production from the CES Selector (2017). Moreover, the experimentally measured electrical energies for manufacturing (in kWh) were converted to oil-equivalent energy by (*i*) multiplying by 3.6 (to shift from kWh to MJ of electricity consumption) and (*ii*) dividing by an energy conversion efficiency of 0.38 (Ashby, 2013 and 2016). The thus-computed primary energy (which is used to present the results in the following sections) should be intended as the amount of energy that would theoretically be necessary for a conventional power station to produce a given amount of electricity (Segers, 2008). Therefore, to account for the proportional contribution of non-renewable and renewable sources in the energy mix, the carbon dioxide equivalent was obtained by considering the greenhouse gas emission intensity of electricity generation (0.285 kg/kWh) for EU-28 (2018), as provided by the European Environmental Agency (EEA, 2020). The inventory data collected to perform the comparative life cycle assessment is detailed hereafter.

3.1. Material production and recycling benefit awarding

Regarding the feedstock material production, most tool steel making is based on Electric Arc Furnace (EAF) melting, followed by secondary metallurgy processes (such as the ladle treatment), recasting and remelting steps. A batch made of both scrap and sponge iron is generally processed and cast into ingots (Morrow et al., 2007), which are then converted into blocks, slabs or bars, through the pre-manufacturing operations of rolling and forging, and heat treatments are then carried out (Voestalpine Böhler Edelstahl GmbH & Co KG, 2018). The use of recycled materials as well as the creation of recyclable materials, such as the chips obtained as a by-product of the machining process or the end-of-life mold insert, represent a net environmental benefit. The so-called ‘Recycled Content Approach’ (RCA) or ‘Substitution Method’ (SM) proposed by Hammond and Jones (2010) could be applied to account for the shared benefits between adjoining product systems. RCA addresses the full benefits of material recycling on the incoming recycled content (which is labelled as R). The SM, on the contrary, computes the recycling credits as a function of the recyclability of the material (r), which typically occurs at different timescales, depending on the type of scrap (Ashby, 2013, pp. 87-92). On the basis of these considerations and previous studies by the authors (Priarone et al., 2019; Campatelli et al., 2020), the here presented analysis was performed by quantifying the cradle-to-gate impact on the present climate, and the potential savings from end-of-life recyclability were computed separately (Hammond and Jones, 2010).

Table 2. Eco-properties of the H13 material, adapted from the CES Selector (2017).

Parameter	Average value	Range
Energy demand for primary material production (ingot), H_V (MJ/kg)	65	± 4.9 %
Carbon footprint for primary material production (ingot), $CO_{2^\circ V}$ (kg/kg)	4.8	± 4.9 %
Energy demand for material recycling, H_R (MJ/kg)	14	± 5.2 %
Carbon footprint for material recycling, $CO_{2^\circ R}$ (kg/kg)	1.1	± 8.7 %
Recycled material fraction in the current supply, R (-)	0.55	± 5.5 %
Energy demand for hot rolling/forming (MJ/kg)	14	± 5.0 %
Carbon footprint for hot rolling/forming (kg/kg)	1.1	± 5.1 %
Material utilization fraction for hot rolling/forming (-)	0.95	± 5.3 %
Energy demand for wire drawing (MJ/kg)	107	± 5.2 %
Carbon footprint for wire drawing (kg/kg)	8.0	± 5.0 %
Material utilization fraction for wire drawing (-)	0.88	± 2.9 %

The average values and the ranges of variability of the main eco-properties of the H13 material were extracted from the CES Selector (2017) database and are listed in Table 2. The embodied energy, E_E (i.e., the primary energy necessary to produce a unit mass of material), and the carbon footprint, $CO_{2\,E}$ (i.e., the carbon dioxide equivalent release to the atmosphere per unit mass of material) of the raw material (i.e., the ingot) were modeled by means of RCA. The well-established $E_E^{RCA} = H_V - R \cdot (H_V - H_R)$ and $CO_{2\,E}^{RCA} = CO_{2\,V} - R \cdot (CO_{2\,V} - CO_{2\,R})$ equations were applied by neglecting the impacts that arise from the disposal of waste material (Hammond and Jones, 2010). Then, in order to compute the energy and carbon footprint of a unit mass of either the workpiece or the wire, the contributions of the pre-manufacturing phases (i.e., workpiece forming or hot rolling plus wire drawing) were added while accounting for the related material waste flows. The latter were estimated as a function of the material utilization fraction (in Table 2), i.e., the mass fraction of material entering the process which remains in the final output. A hot rolling was considered as the process to form ingots and blooms into slabs, plates, sheets and sections, which may then be used in other shape-modifying processes, such as wire drawing. The results are summarized in Table 3. These results were obtained by considering a worst-case scenario (i.e., the highest impact of each unit process, the lowest recycled material fraction and the lowest material utilization fraction for pre-manufacturing) and a best-case scenario (i.e., the lowest impact of each unit process, the highest recycled material fraction and the highest material utilization fraction for pre-manufacturing). Such a choice justifies the higher data variability than in Table 2. The thus-computed values of the workpiece production are coherent with those of Morrow et al. (2007), who considered data from the U.S. Department of Energy. As for workpiece production, they quantified (*i*) a specific electricity consumption of 20 MJ/kg (which results in 52.6 MJ/kg when a primary-to-secondary energy conversion efficiency of 0.38 is assumed) and (*ii*) CO_2 emissions of approximately 3 kg/kg. Lastly, in addition to impacts on the present climate, the potential (future) credits due to the recyclability of fraction r of the material were assessed. The approach detailed in Hammond and Jones (2010) was applied. The r value ranges were assumed by considering the recycling efficiency of different types of waste materials, according to Ingarao et al. (2018).

Table 3. Environmental impact of the incoming feedstock materials.

Parameter	Average value	Range
Embodied (primary) energy per unit mass of workpiece (MJ/kg)	54	± 14.1 %
Carbon footprint per unit mass of workpiece (kg/kg)	4.0	± 14.6 %
Embodied (primary) energy per unit mass of wire (MJ/kg)	184	± 11.4 %
Carbon footprint per unit mass of wire (kg/kg)	13.7	± 11.4 %

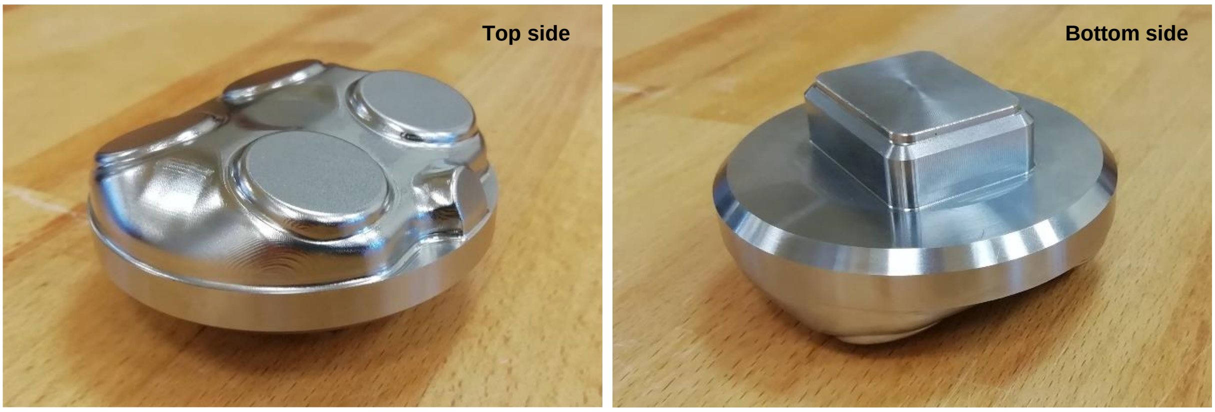

Figure 7. Mock-up of the H13 mold insert assumed as the case study.

3.2. Manufacturing of a new mold insert

A new mold insert is usually manufactured, during its first life, by milling it from a massive workpiece. A total amount of 761 g of chips was removed from an 80-mm diameter round bar weighing 1568 g by means of subsequent rough, semi-finish and finish machining operations. The process was first carried out on the bottom side (Figure 7), the part was then repositioned on the piece-holder table and the features on the top side were machined. The manufacturing time and energy requirements were experimentally measured, and the results are summarized in Table 4. Figure 8 shows, as an example, the power demand versus time profile for the cross-hatch finishing of the top side of the mold insert. Moreover, in addition to the operational mode (that is, the removal of the exceeding material in the shape of chips), the non-productive times related to the setup of the machine, the handling/positioning/loading/unloading of the workpiece, as well as to the tool change were included to provide a complete characterization of the unit-process. The same methodology was followed throughout the whole analysis detailed hereafter.

Table 4. Process time and electric energy demand for the milling of a new mold insert.

Operation	Machined material (g)	Process time (min)	Electric energy (kWh)
Setup / Idle operational mode	-	10.0	0.33
Bottom side, roughing + finishing	432	52.0	2.15
Top side, roughing	318	69.9	2.89
Top side, Z-level semi-finishing	8	73.4	2.91
Top side, Cross-hatch finishing	3	12.4	0.62
Total	**761**	**217.7**	**8.90**

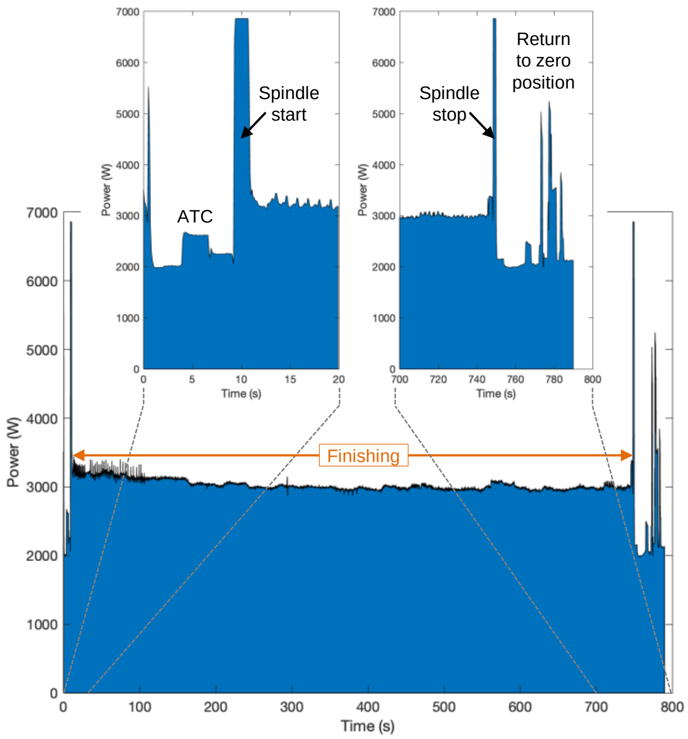

Figure 8. Power versus time curve during cross-hatch finishing of the top side of the mold insert.

The machining of a single mold insert lasted 3.6 h and required 8.90 kWh of electric energy, 3.7% of which was consumed in the idling operational mode. The process parameters depend on the strict dimensional and surface finish requirements of the features being machined. This technological constraint affected both the Material Removal Rate (MRR), which ranged from 0.5 kg/h to 0.007 kg/h, and the Specific (electric) Energy Consumption (SEC), which ranged from 5.0 kWh/kg to 363.8 kWh/kg (Kara and Li, 2011). It is worth mentioning that an optimization of the process could be introduced in the case of the mass production of the insert, but the here adopted setup is consistent with operation on a single component whenever conservative parameters are preferred.

3.3. Repair of the mold insert

The wear mechanism of the mold insert during the use phase is mainly related to micro-cracking of the top surface, which in turn may subsequently lead to a sudden breakage of the insert with macroscopic fractures. Therefore, the appearance of micro-cracks requires the replacement of the mold insert or its repair (which is analyzed in this Section) to avoid catastrophic failures of the component. The variation of the mass of the mold inserts in the use phase, due to the formation of micro-chipping and debris, is usually negligible; thus, it was not considered in this research. The repair process in the hybrid additive-subtractive machine required three main phases: (*i*) substrate preparation; (*ii*) WAAM deposition; and (*iii*) post-repair finishing. In addition, a thermal treatment may also be required between phase (*ii*) and phase (*iii*), according to Section 2.2, and its contributions to the cumulative energy demand and CO_2 emissions were verified on the basis of the available literature.

3.3.1. Substrate preparation

A milling operation was required to prepare the substrate prior to the material deposition by means of WAAM. The experimentally acquired manufacturing time and electric energy requirements are listed in Table 5. The substrate preparation took 0.67 h and required 1.61 kWh of electric energy, 10.6% of which was consumed in the idling operational mode. The MRR was 0.08 kg/h for roughing and 0.03 kg/h for finishing, which resulted in a Specific (electric) Energy Consumption of 29.5 kWh/kg and 87.5 kWh/kg, respectively.

Table 5. Process time and electric energy demand for preparation of the substrate.

Operation	Machined material (g)	Process time (min)	Electric energy (kWh)
Setup / Idle operational mode	-	5.0	0.17
Substrate preparation, Roughing	37	26.5	1.09
Substrate preparation, Finishing	4	8.8	0.35
Total	**41**	**40.3**	**1.61**

3.3.2. WAAM deposition

The repair process was performed by exploiting the CMT technology. The material deposition was preceded by pre-heating of the insert and was followed by a post-WAAM cooling step, the impacts of which were accounted for as follows.

- **Insert pre-heating.** The impact of the pre-heating phase (prior to the WAAM process) was assessed by considering a 30-liter furnace for laboratory/small-scale production (Berzi et al., 2019). Such a furnace operates at 1000 W for 60 minutes in a typical cycle to heat the chamber, and the power demand is then reduced to 560 W for 25 minutes to heat the part to an imposed temperature of 300°C. In the worst-case scenario (i.e., when a single insert is heated per batch, and the furnace is therefore only filled to less than 10% of its capacity), the here-estimated electric energy per unit is 1.23 kWh. This assumption may be considered realistic, particularly when all the repair operations (including material removal) have to be scheduled in a single additive/subtractive integrated machine, which therefore becomes the bottleneck of the system.
- **Material deposition.** The electric energy consumption for the deposition of the H13 layer on the pre-machined surface (weighing 156 g, which corresponds to a wire consumption of 25.5 m) was measured as 0.29 kWh. Of this value, 55% was due to the deposition head (0.16 kWh), while the remaining part was due to the consumption of the machine tool and the auxiliary equipment (0.13 kWh). The selected process parameters resulted in an average deposition rate of 2.28 kg/h; the deposition time was 4.1 min. Therefore, the specific energy consumption for the deposition phase alone was 1.86 kWh/kg (i.e., 6.7 MJ of electric energy per unit mass of deposited material), which is coherent with other literature sources regarding CMT processes (Priarone et al., 2020; Catalano et al., 2019, and references therein). In addition, the energy requirements during the setup time were included in the assessment. The setup time was quantified as 8 min (including the handling/positioning of the part as well as the automatic tool change and the connection of the wiring to the deposition head), while the average power demand of the hybrid machine was 2 kW when idling. Thus, the total electric energy per processed unit was 0.56 kWh, and the contributions other than the deposition phase were approximately half of the total.
- **Post-WAAM cooling.** After material deposition, the part is cooled in air, and no contributions to energy consumption or to the related carbon dioxide emissions are therefore expected. Conversely, this dead time could affect both the productivity and overall manufacturing costs, which have not been considered in the boundaries of this research.

3.3.3. Heat treatment

A heat treatment after WAAM may be needed to improve the structure of the material, to refine the grain, and/or to reduce stresses and hardness for machining. Therefore, although a heat treatment was not carried out experimentally in this research, an annealing process was included in the environmental assessment to verify whether its impacts would have been significant for the whole analysis. An estimation for the electric energy consumption, equal to 1.19 MJ (or 0.33 kWh) per kg of treated material, was obtained from Morrow et al. (2007). The mass of the semi-finished part that had to be treated was 922 g, and the extra-energy for annealing was therefore 0.30 kWh.

3.3.4. Post-repair finishing

The whole finishing operation necessary to restore the original geometry of the top side of the mold required approximately 1.5 h and 4.05 kWh, as reported in Table 6. The imposed MRR ranged from 0.21 kg/h, when roughing, to 0.02 kg/h when finishing. Therefore, the resultant SEC varied from 11.6 kWh/kg to 206.7 kWh/kg.

Table 6. Process time and electric energy demand for post-repair finishing.

Operation	Machined material (g)	Process time (min)	Electric energy (kWh)
Setup / Idle operational mode	-	5.0	0.17
Post-repair machining, Roughing	100	28.0	1.16
Post-repair machining, Z-level semi-finishing	12	47.0	2.10
Post-repair machining, Cross-hatch finishing	3	12.4	0.62
Total	**115**	**92.4**	**4.05**

3.4. Consumables

In addition to the electricity consumption for each unit process, which has been quantified in Section 3.2 and Section 3.3, the environmental impacts due to the consumables (such as the shielding gas and the cutting tools) were included in the analysis. The WAAM process for the repair operation consumed 65 normal liters of the Pulsarc 102 M12 gas, which is a mixture made mainly of argon (98%). The consumption of argon, even though the protective gas was not re-captured during material deposition, due to its low embodied energy (i.e., 0.7 MJ/kg, according to Kamps et al., 2018), was assumed to be negligible with respect to the total energy required for the complete manufacturing approach (Campatelli et al., 2020). All the machining operations were performed under dry cutting conditions. Apart from the undisputed environmental advantages, as reviewed by Weinert et al. (2004), this choice was also motivated by the fact that, in the case of a hybrid additive-subtractive machine, problems could arise in the management of the process waste when cutting fluids and dust/residues of deposited material coexist. On the other hand, tool wear in dry cutting of difficult-to-machine materials could have a significant impact on the economic and environmental performance of the machining processes (Priarone et al., 2018). In this context, experimental trials aimed at obtaining Taylor's curves could be useful. However, when complex three-dimensional features have to be produced via a 5-axis CNC machine, the tool-workpiece engagement conditions might vary during cutting, and the adoption of simplified models and assumptions could lead to an over- or under-estimation of the actual tool life. For the case study, the machining operations were carried out by means of TiAlN-coated tungsten carbide mills. NS IE-0098 10-mm diameter end mills (weighing 88 g) and MACH2 25SF R2x10 4-mm diameter ball-end mills (weighing 13 g), provided by NS tools, were used for roughing and (semi-)finishing, respectively. The tools were replaced after the production of 5 repaired mold inserts. When the same tools were applied to manufacture a new mold, 3 mold inserts were produced. All the environmental impacts were considered for the embodied energy and carbon footprint for the primary production of tungsten carbide, which were assumed to be 549-605 MJ/kg (which is slightly higher than the value of 400 MJ/kg applied in other studies) and 36-40 kg/kg (CES Selector, 2017). No benefits deriving from material recycling, or the possibility of re-sharpening the cutting edges, were considered. Therefore, the resultant primary energy requirements, due to cutting tool consumption, were 11.1 - 12.2 MJ for the repaired mold insert, and 18.5 - 20.4 MJ for the brand-new mold insert. Similarly, the equivalent carbon dioxide emissions were 0.7 - 0.8 kg and 1.2 - 1.3 kg, respectively.

4. Results and discussion

Figure 9 shows the results of a comparative assessment as a function of the primary energy requirements (Fig. 9*a* and 9*b*) and equivalent CO_2 emissions (Fig. 9*c* and 9*d*). The graphs in Figure 9 are designed according to the boundaries of the study for 'Scenario A' and 'Scenario B', which have been defined in Figure 6. The solid bars plot the average values (which are also reported in the labels), while the error bars define the range from the worst-case scenario to the best-case one with respect to the uncertainty in the input data. Regarding the production of the incoming feedstock materials - i.e., the workpiece and the wire - the benefits related to the recycled material content in the actual supply were included in the energy and carbon contributions. In addition, the potential energy and carbon savings that arise from EoL recyclability were added as separate bars (Hammond and Jones, 2010). For the sake of simplicity, all the benefits due to the recyclability of either the chips or the bulk material have been grouped together. However, it is worth remarking that primary (or 'new') scraps deriving from manufacturing processes can be recycled before secondary (or 'old') material scraps, which only become available when the product reaches the end of its useful life (Ashby, 2013, pp. 85-92).

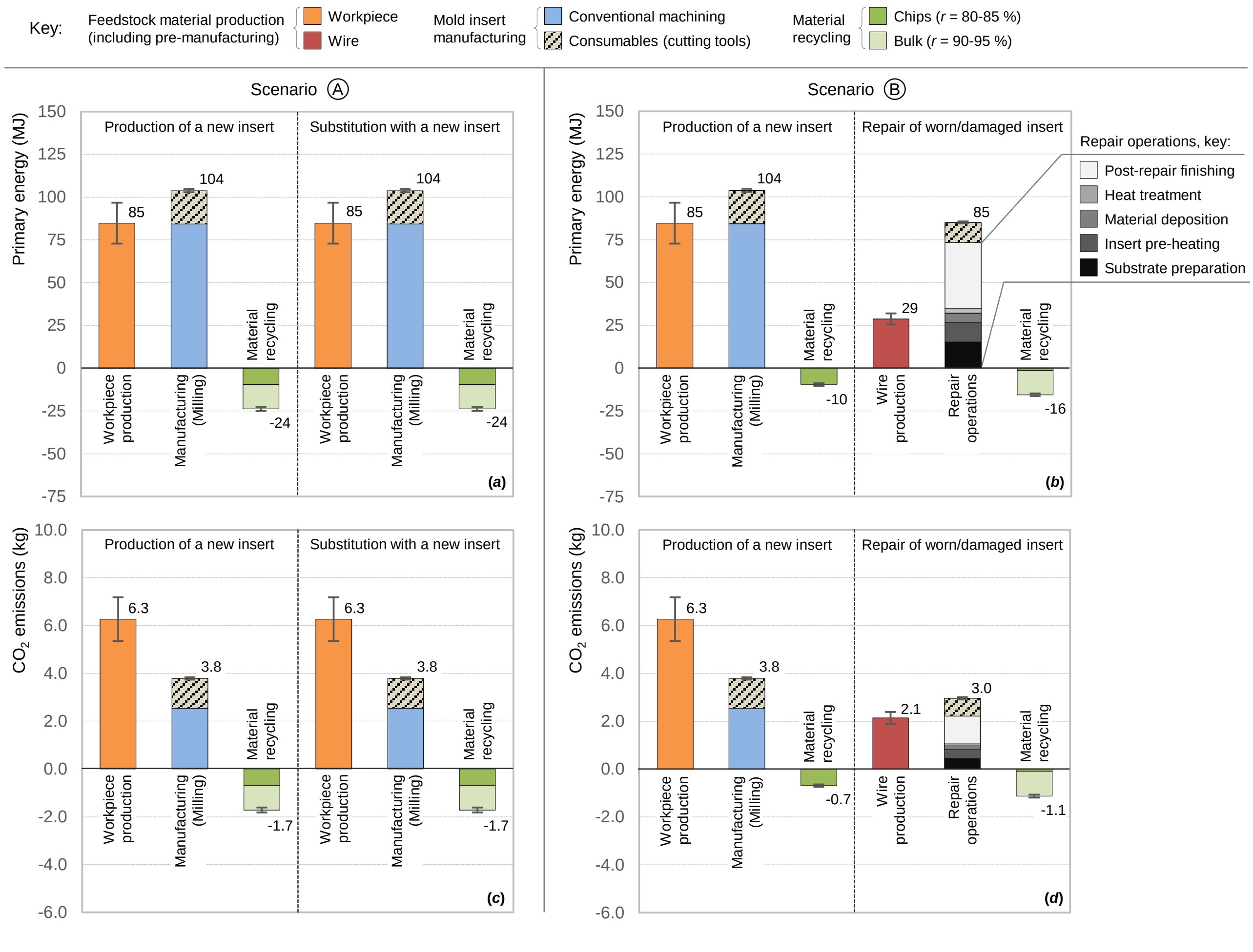

Figure 9. Cumulative energy demand (*a*, *b*) and carbon dioxide emissions (*c*, *d*) for both of the considered scenarios.

'Scenario A' refers to the replacement of a worn/damaged insert with a brand new one (Figure 6). In the case of no changes in the material supply, recycling policies or manufacturing cycle, the environmental impact of each single product could theoretically be assumed as constant over time. As a result, no variations in the impacts of the life cycle phases between the production of a new insert and its substitution with a brand new one are assumed (as shown in Fig. 9*a* and 9*c*). Thus, the average energy demand and CO_2 emissions for the whole 'Scenario A' (i.e., the production of the mold insert plus its replacement) were quantified as 330 MJ and 16.8 kg, respectively. For the case of 'Scenario B', which instead allows for the subsequent reuse of the repaired mold insert, these values are reduced to 277 MJ (- 16.1 %) and 13.4 kg (- 20.2 %). The worn/damaged insert that has to be repaired maintains the energy incorporated in the material of which it is made.

Thus, the benefits derived from the end-of-life recyclability of the bulk material are postponed (Fig. 9*b* and 9*d*). A smaller amount of material (- 90.1 %) is consumed for the repair operations than for the insert substitution scenario. According to Figure 6, 156 g of H13 wire was needed to compensate for the mass of chips removed during the pre- and post-WAAM machining. The results highlight that, although the embodied energy and carbon footprint per unit mass of wire are approximately 3.5 times higher than those of the workpiece (cf. Table 3), the impact of feedstock material production - including the pre-manufacturing - is reduced by two thirds (e.g., 29 MJ versus 85 MJ; 2.1 kg versus 6.3 kg of CO_2). As for the manufacturing phase, the contributions in Figure 9 are mainly driven by the electric energy consumption of the equipment. Since (*i*) these operations have been experimentally characterized, and (*ii*) the data variability has only been addressed to the consumable resources, the differences between the best-case and worst-case scenarios in Figure 9 were small. Overall, despite the necessary number of unit-steps, the repair-based approach required less primary energy than traditional machining. Moreover, since the primary energy demand relies mostly on electric energy consumption, the related CO_2 emissions were consequently lower. Among the different repair steps, the contribution of the material deposition by means of WAAM accounted for less than one tenth of the total, for both of the here considered metrics. This evidence is partially related to the low specific energy consumption of CMT, which has proved to be an energy-efficient technique for repair purposes (Selvi et al., 2018). Moreover, the contribution of the annealing treatment (which was theoretically included on the basis of literature data) was not significant in this analysis. On the other hand, the machining processes dominate the impact of manufacturing, for both 'Scenario A' and 'Scenario B'. This indication is consistent with the results of the comparative LCA-based study carried out by Wilson et al. (2014) on repair techniques. When such welding processes as GTAW and PTAW were employed, the ratios between the electric energy consumption of the deposition system and that calculated for a 5-axis CNC machine were comparable to the ones obtained here. Moreover, the impact of additive or subtractive processes also depends on other factors. On the one hand, it depends on the choice of the employed techniques and the relative equipment. Wilson et al. (2014), for instance, highlighted that the energy demand of repair operations conducted by means of Laser Direct Deposition (LDD) was one order of magnitude higher than that of GTAW or PTAW. On the other hand, the relative impact of CNC milling and DMD-based approaches can differ to a great extent as a function of the solid-to-cavity ratio (Morrow et al., 2007).

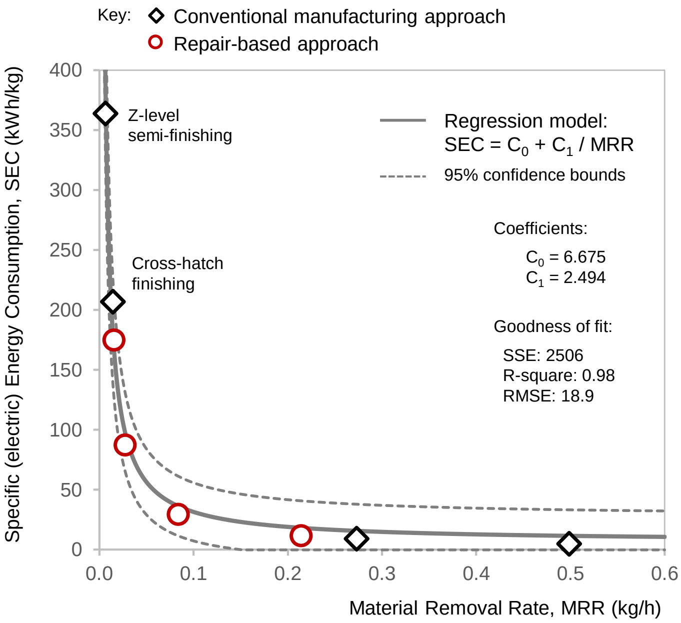

Figure 10. SEC versus the MRR curve for material removal operations.

4.1. Impact of the material removal operations

The unit-process energy consumption of machining is mainly related to the architecture of the machine itself, with only a slight impact being due to the cutting process (Behrendt et al., 2012). According to Kara and Li (2011), each machine tool is expected to be characterized by a SEC versus MRR curve. Overall, the higher the material removal rate is, the lower the specific energy consumption. Figure 10 plots the experimental values that correlate SEC and MRR for the different material removal operations involved in the present case study (which have already been detailed in Section 3). The variations in the SEC values differ by at least one order of magnitude. The Z-level semi-finishing and the cross-hatch finishing (the latter being common to both 'Scenario A' and 'Scenario B') were identified as the most energy-intensive processes per unit mass of removed chips. This experimental evidence is consistent with available literature sources (e.g., Kara and Li, 2011; Li and Kara, 2012), as well as with experiments performed by the authors on similar systems (Campatelli et al., 2020). Moreover, Morrow et al. (2007) quantified the energy demand of roughing operations for H13 machining as 24 MJ/kg, while the energy demand for finishing was 25 times higher. The SEC = $C_0 + C_1$/MRR model was applied, and its coefficients were obtained by means of regression analysis (Figure 10). It is worth mentioning that the process parameters adopted in this study have not been optimized in view of maximizing the energy efficiency. In the present case, the authors preferred to resort to precautionary values that would be able to satisfy the strict surface requirements necessary to create the mock-up of the mold insert. Therefore, when transitioning from a lab-scale to an industrial-scale application, an optimization of the machining process parameters that allows an increase in MRR can be expected to result in smaller contributions of the material-removal unit processes (Priarone et al., 2020). However, considering that the higher share is due to the finishing operations (which, in turn, are constrained by the geometrical product specifications), the conventional machining approach (Scenario A) should still be the most expensive in terms of energy consumption and CO_2 emissions.

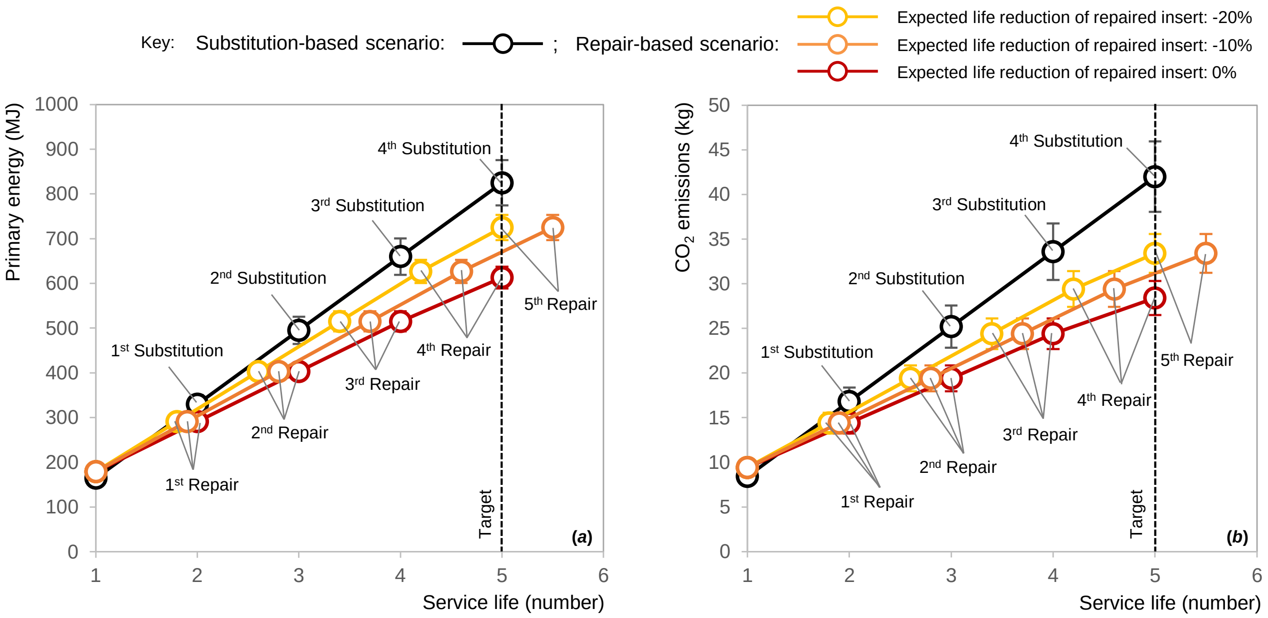

Figure 11. Multiple repair scenario: variations in the cumulative energy demand and CO_2 emissions over time.

4.2. Multiple repair loops

The results presented in Figure 9 were obtained considering the study boundaries defined in Figure 6. Therefore, the discussion in the previous sections was limited to the scenarios in which a newly produced mold insert is either replaced or repaired at the end of its service life. The circular economy requires techniques that allow the lifespan of products to be extended, their disposal to landfills to be postponed once they reach the end of their first life, and the material loop to be closed by means of reuse, remanufacturing and recycling strategies. Therefore, Multiple Life Cycles (MLCs) should be forecasted (King et al., 2006; Wu et al., 2014). When multiple repair loops are technologically feasible, the expected environmental impact reduction could be amplified over time, as a function of the number of remanufacturing cycles (Gu et al., 2020). Therefore, a comparative assessment was carried out by shifting from a product-oriented analysis to a function-oriented one. The function of a mold insert is to allow a batch of automotive cylinders to be die-cast. If the total production volume of cylinders is known, the number of needed inserts can be calculated. For explanatory purposes, Figure 11 was prepared under the assumption that 5 brand-new mold inserts (with an equal duration of the service life) are necessary to achieve the production target. The cumulative trends of the environmental performance metrics increase linearly with time for the substitution-based scenario, since the primary energy in a brand-new insert (165 MJ, according to Figure 9) as well as the related emissions (8.4 kg of CO_2) have to be accounted for each insert replacement. The obtained cumulative values are lower in the case of multiple repair loops. This is due to both the lower consumption of primary material (although the recycling of the bulk insert material is postponed), as a result of the cascading effect (Gu et al., 2020), and the lower requirements of repair operations. If the service life of the repaired insert is assumed to be identical to that of the brand-new insert, the total energy consumption and CO_2 emissions are reduced by 26 and 32%, respectively, to satisfy the same production target. Whenever the life of the repaired component is shorter, the repair operations have to be anticipated and their frequency has to be increased. However, despite the consequent increase in the performance assessment metrics (as shown in Figure 11), the repair-based scenario appears to be sustainable up to a threshold value for the expected service life reduction (i.e., approximately -30% in the case study).

5. Conclusions

A procedure to repair a mold insert for use in the casting of aluminum cylinder heads for internal combustion engines has been developed and analyzed in this research to quantitatively support the literature that claims that remanufacturing, reconditioning and repair are the best strategies to recover the value of the resources involved in manufacturing a product, rather than scrapping and recycling it at the end of its service life. A comparative cradle-to-gate life-cycle energy and carbon footprint assessment was carried out considering two scenarios: the replacement of a worn mold with a brand new one and the repair of the mold to extend its lifespan at the end of the first life of the product. A hybrid additive-subtractive center, based on CMT technology, was employed for the repair-based scenario. To better understand and assess the role of AM in establishing Circular Economy principles, and the related potential savings, the same analyses was extended to multiple repairs which guaranteed the function of the mold. Most of the process data were acquired during experimental tests to reduce the uncertainty of the analysis input data. The analysis results show that even the most conservative scenarios among those considered highlighted the effectiveness of the repair procedure. The environmental impact analysis demonstrated how the repair-based approach, thanks to a reduction in the material usage and cumulative energy requirements, could be an efficient solution to support the transition toward greener manufacturing approaches. The overall material consumption is reduced, and this is particularly important, especially when a high-impact material is required for the operation. The greatest contribution to the environmental impact resulted to be the machining phase, as a result of two main concurrent factors. First, the WAAM deposition technology used to re-create the worn surface (i.e., CMT) is quite efficient and, unlike other AM solutions, has a lower energy consumption. Second, the strict surface finish requirements that have to be achieved on the machine tool required a particularly long time, and thus negatively influenced the energy consumption of this phase. On the one hand, this result can be associated with the choice of precautionary values for the cutting parameters to satisfy the strict surface finishing requirements. On the other hand, a predominance of the machining phase has also been witnessed in other literature studies, even when coupled with high-demanding deposition processes (Wilson et al. 2014). As for a longer-term production perspective (common to such sectors as the automotive one), multiple repair loops could boost the efficiency of the process scenarios. Even when considering different reductions in the lifespan of an insert, the repair-based approach resulted to be a better solution to grant a relevant reduction in the environmental impact than the substitution-base scenario. In addition, this research has confirmed that the use of a hybrid additive-subtractive production center could streamline the repair process by ensuring that the reported layer has material characteristics that comply with the reuse of the product. Moreover, its capability of carrying out all the steps required for repairs with the same fixturing on a single machine and without the need to move or reposition the metal part may be envisaged as a sound industrial solution to smoothly repair high-value components. This technological solution, coupled with a transitioning from a lab-scale- to an industrial-scale-based choice and optimization of the machining process parameters (which would result in to an increase in MRR and to lower impacts due to the material-removal unit processes) is expected to gradually lead to the implementation of Circular Economy principles within the industrial manufacturing context.

Acknowledgments

Part of this research was funded by the European Union's Horizon 2020 research and innovation programme, under grant agreement No. 721267, the Manunet III - RetroFix project (www.retrofix-project.net). The authors wish to thank Aurrenak S. Coop for performing the metallographic analysis and the technical feedback concerning the quality of the repair process, as well as the Machine Tool Technology Research Foundation (MTTRF) for loaning the machine tool (DMG MORI DMU 75 MonoBlock) used for the experimental tests.

Declaration of competing interest

The authors declare that they have no known competing financial interests or personal relationships that could have appeared to influence the work reported in this paper.

References

Allwood, J.M., Cullen, J.M., 2011. Sustainable Materials With Both Eyes Open: Future Buildings, Vehicles, Products and Equipment - Made Efficiently and Made with Less New Material. London.

Ashby, M.F., 2013. Materials and the Environment: Eco-informed Material Choice. ISBN: 978-0-12-385971-6, second ed. Butterworth Heinemann/Elsevier, Waltham, MA, USA and Kidlington, Oxford, UK.

Ashby, M.F., 2016, Materials and sustainable development, Butterworth- Heinemann, Kidlington, Oxford, UK, ISBN: 978-0-08-100176-9.

Bambach, M.D., Bambach, M., Sviridov, A., Weiss, S., 2017. New process chains involving additive manufacturing and metal forming - A chance for saving energy? Procedia Eng. 207, 1176–1181. https://doi.org/10.1016/j.proeng.2017.10.1049

Bandari, Y., Ding, J., Martina, F., Williams, S., 2015. Additive Manufacture of Large Structures: Robotic or CNC Systems?. 26th Int. Solid Free. Fabr. Symp. Austin, Texas 1, 17–25. https://doi.org/10.1017/CBO9781107415324.004

Behrendt T., Zein A., Min, S., 2012. Development of an energy consumption monitoring procedure for machine tools: CIRP Ann.-Manuf. Techn. 61, 43-46. https://doi.org/10.1016/j.cirp.2012.03.103

Bennett, J., Garcia, D., Kendrick, M., Hartman, T., Hyatt, G., Ehmann, K., You, F., Cao, J., 2019. Repairing Automotive Dies with Directed Energy Deposition: Industrial Application and Life Cycle Analysis. J. Manuf. Sci. Eng. Trans. ASME 141. https://doi.org/10.1115/1.4042078

Berzi, L., Antoni Dattilo, C., Del Pero, F., Delogu, M., Gonzalez, M.I., 2019. Reduced use of rare earth elements for permanent magnet generators: preliminary results from NEOHIRE project. Procedia Structural Integrity 24, 961-977. https://doi.org/10.1016/j.prostr.2020.02.084

Bi, G., Gasser, A., 2011. Restoration of nickel-base turbine blade knife-edges with controlled laser aided additive manufacturing. Phys. Procedia 12, 402–409. https://doi.org/10.1016/j.phpro.2011.03.051

Campatelli, G., Montevecchi, F., Venturini, G., Ingarao, G., Priarone, P.C., 2020. Integrated WAAM-Subtractive Versus Pure Subtractive Manufacturing Approaches: An Energy Efficiency Comparison. Int. J. Precis. Eng. Manuf. - Green Technol. 7. https://doi.org/10.1007/s40684-019-00071-y

Catalano A.R., Lunetto, V., Priarone, P.C., Settineri, L., 2019. A Survey on Energy Efficiency in Metal Wire Deposition Processes. Smart Innovation. Systems and Technologies 155, 311-322. https://doi.org/10.1007/978-981-13-9271-9_26.

CES Selector, 2017. Update 1, version 17.2.0 (Granta Design Limited, the UK).

Chen, C., Wang, Y., Ou, H., He, Y., Tang, X., 2014. A review on remanufacture of dies and moulds. J. Clean. Prod. 64, 13–23. https://doi.org/10.1016/j.jclepro.2013.09.014

Chen, D., Heyer, S., Ibbotson, S., Salonitis, K., Steingrímsson, J.G., Thiede, S., 2015. Direct digital manufacturing: Definition, evolution, and sustainability implications. J. Clean. Prod. 107, 615–625. https://doi.org/10.1016/j.jclepro.2015.05.009

Colorado, H.A., Velásquez, E.I.G., Monteiro, S.N., 2020. Sustainability of additive manufacturing: the circular economy of materials and environmental perspectives. J. Mater. Res. Technol. 9, 8221–8234. https://doi.org/10.1016/j.jmrt.2020.04.062

Cruz Sanchez, F.A., Boudaoud, H., Camargo, M., Pearce, J.M., 2020. Plastic recycling in additive manufacturing: A systematic literature review and opportunities for the circular economy. J. Clean. Prod. 264, 121602. https://doi.org/10.1016/j.jclepro.2020.121602

Cunningham, C.R., Flynn, J.M., Shokrani, A., Dhokia, V., Newman, S.T., 2018. Strategies and processes for high quality wire arc additive manufacturing. Addit. Manuf. 22, 672–686. https://doi.org/10.1016/j.addma.2018.06.020.

Despeisse, M., Ford, S., 2015. The Role of Additive Manufacturing in Improving Resource Efficiency and Sustainability, in: IFIP Advances in Information and Communication Technology. pp. 129–136. https://doi.org/10.1007/978-3-319-22759-7_15

Despeisse, M., Ford, S., Viljakainen, A., 2015. Product life extension through additive manufacturing, the business model implications. https://doi.org/10.13140/RG.2.1.4561.9282

Despeisse, M., Yang, M., Evans, S., Ford, S., Minshall, T., 2017. Sustainable Value Roadmapping Framework for Additive Manufacturing. Procedia CIRP 61, 594–599. https://doi.org/10.1016/j.procir.2016.11.186

Dilberoglu, U.M., Gharehpapagh, B., Yaman, U., Dolen, M., 2017. The Role of Additive Manufacturing in the Era of Industry 4.0. Procedia Manuf. 11, 545–554. https://doi.org/10.1016/j.promfg.2017.07.148

Ding, D., Pan, Z., Cuiuri, D., Li, H., 2015. A multi-bead overlapping model for robotic wire and arc additive manufacturing (WAAM). Robot. Comput. Integr. Manuf. 31, 101-110. https://doi.org/10.1016/j.rcim.2014.08.008

EEA (European Environment Agency, 2020. Greenhouse gas emission intensity of electricity generation. Available at: https://www.eea.europa.eu/data-and-maps/daviz/co2-emission-intensity-6#tab-googlechartid_googlechartid_chart_111_filters=%7B%22rowFilters%22%3A%7B%7D%3B%22columnFilters%22%3A%7B%22pre_config_date%22%3A%5B2018%5D%7D%3B%22sortFilter%22%3A%5B%22index_2018%22%5D%7D (Last accessed on March 22, 2021).

Ellen MacArthur Foundation, 2013. Towards the Circular Economy, Ellen MacArthur Foundation. Available at: https://www.ellenmacarthurfoundation.org/assets/downloads/publications/Ellen-MacArthur-Foundation-Towards-the-Circular-Economy-vol.1.pdf (Last accessed on March 22, 2021).

Emmelmann, C., Sander, P., Kranz, J., Wycisk, E., 2011. Laser additive manufacturing and bionics: Redefining lightweight design. Phys. Procedia 12, 364–368. https://doi.org/10.1016/j.phpro.2011.03.046

Ford, S., Despeisse, M., 2016. Additive manufacturing and sustainability: an exploratory study of the advantages and challenges. J. Clean. Prod. 137, 1573–1587. https://doi.org/10.1016/j.jclepro.2016.04.150

Ford, S., Despeisse, M., Viljakainen, A., 2015. Extending product life through additive manufacturing : The sustainability implications. https://doi.org/10.13140/RG.2.1.4561.9282

Frischknecht, R., Wyss, F., Büsser Knöpfel, S., Lützkendorf, T., Balouktsi, M., 2015. Cumulative energy demand in LCA: the energy harvested approach. International Journal of Life Cycle Assessment 20/7, 957-969. https://doi.org/10.1007/s11367-015-0897-4

Ge, J., Ma, T., Chen, Y., Jin, T., Fu, H., Xiao, R., Lei, Y., Lin, Y., 2019. Wire-arc additive manufacturing H13 part: 3D pore distribution, microstructural evolution, and mechanical performances. J. Alloys Compd. 783, 145–155. https://doi.org/10.1016/j.jallcom.2018.12.274

Gu, Y., Zhou, G., Wu, Y., Xu, M., Chang, T., Gong, Y., Zuo, T., 2020. Environmental performance analysis on resource multiple-life-cycle recycling system: Evidence from waste pet bottles in China. Resour. Conserv. Recycl. 158, 104821. https://doi.org/10.1016/j.resconrec.2020.104821

Hammond, G., Jones, C., 2010. Inventory of Carbon and Energy (ICE), Annex B: How to Account for Recycling a Methodology for Recycling. The University of Bath, Bath, UK.

Hinojos, A., Mireles, J., Reichardt, A., Frigola, P., Hosemann, P., Murr, L.E., Wicker, R.B., 2016. Joining of Inconel 718 and 316 Stainless Steel using electron beam melting additive manufacturing technology. Mater. Des. 94, 17–27. https://doi.org/10.1016/j.matdes.2016.01.041

Huang, R., Riddle, M., Graziano, D., Warren, J., Das, S., Cresko, J., Masanet, E., 2015. Energy and Emissions Saving Potential of Additive Manufacturing: The Case of Lightweight Aircraft Components. J. Clean. Prod. https://doi.org/10.1016/j.jclepro.2015.04.109

IEA, CO_2 Emissions from Fuel Combustion 2018: Highlights (Paris: International Energy Agency, 2018) p.101.

Ijomah, W.L., McMahon, C.A., Hammond, G.P., Newman, S.T., 2007. Development of design for remanufacturing guidelines to support sustainable manufacturing. Robot. Comput. Integr. Manuf. 23, 712–719. https://doi.org/10.1016/j.rcim.2007.02.017

Ingarao, G., Priarone, P.C., Deng, Y., Paraskevas, D., 2018. Environmental modelling of aluminium based components manufacturing routes: Additive manufacturing versus machining versus forming, J. Clean. Prod. 176, 261-275, https://doi.org/10.1016/j.jclepro.2017.12.115

Jawahir, I.S., Bradley, R., 2016. Technological Elements of Circular Economy and the Principles of 6R-Based Closed-loop Material Flow in Sustainable Manufacturing. Procedia CIRP 40, 103–108. https://doi.org/10.1016/j.procir.2016.01.067

Kaierle, S., Overmeyer, L., Alfred, I., Rottwinkel, B., Hermsdorf, J., Wesling, V., Weidlich, N., 2017. Single-crystal turbine blade tip repair by laser cladding and remelting. CIRP J. Manuf. Sci. Technol. 19, 196–199. https://doi.org/10.1016/j.cirpj.2017.04.001

Kamps, T., Lutter-Guenther, M., Seidel, C., Gutowski, T., Reinhart, G., 2018. Cost- and energy-efficient manufacture of gears by laser beam melting. CIRP Journal of Manufacturing Science and Technology 21, 47-60. https://doi.org/10.1016/j.cirpj.2018.01.002.

Kara, S., Li, W., 2011. Unit process energy consumption models for material removal processes. CIRP Annals - Manufacturing Technology 60/1, 37-40. https://doi.org/10.1016/j.cirp.2011.03.018

Khorram Niaki M., Torabi, S.A., Nonino, F., 2019a. Why manufacturers adopt additive manufacturing technologies: The role of sustainability. J. Clean. Prod. 222, 381–392. https://doi.org/10.1016/j.jclepro.2019.03.019

Khorram Niaki, M., Nonino, F., Palombi, G., Torabi, S.A., 2019b. Economic sustainability of additive manufacturing: Contextual factors driving its performance in rapid prototyping. J. Manuf. Technol. Manag. 30, 353–365. https://doi.org/10.1108/JMTM-05-2018-0131

King, A.M., Burgess, S.C., Ijomah, W., McMahon, C.A., 2006. Reducing waste: Repair, recondition, remanufacture or recycle? Sustain. Dev. 14, 257–267. https://doi.org/10.1002/sd.271

Klahn, C., Leutenecker, B., Meboldt, M., 2014. Design for additive manufacturing - Supporting the substitution of components in series products. Procedia CIRP 21, 138–143. https://doi.org/10.1016/j.procir.2014.03.145

Legesse, F., Kapil, S., Vithasth, H., Karunakaran, K.P., 2018. Additive manufacturing of H13 tooling element with conformal cooling channel using MIG cladding, Int. J. Rapid Manuf. 7(1). https://doi.org/10.1504/IJRAPIDM.2018.089725

Leino, M., Pekkarinen, J., Soukka, R., 2016. The role of laser additive manufacturing methods of metals in repair, refurbishment and remanufacturing - Enabling circular economy. Phys. Procedia 83, 752–760. https://doi.org/10.1016/j.phpro.2016.08.077

Lewis, S.R., Lewis, R., Fletcher, D.I., 2015. Assessment of laser cladding as an option for repairing/enhancing rails. Wear 330–331, 581–591. https://doi.org/10.1016/j.wear.2015.02.027

London, M.B., Lewis, G.M., Keoleian G.A., 2020. Life Cycle Greenhouse Gas Implications of Multi Jet Fusion Additive Manufacturing. ACS Sustain. Chem. Eng. 8 (41), 15595-15602. https://doi.org/10.1021/acssuschemeng.0c04845

Li, W., Kara, S., 2011. An empirical model for predicting energy consumption of manufacturing processes: a case of turning process. Proc. Inst. Mech. Eng., Part B 225(9), 1636-1646. https://doi.org/10.1177/2041297511398541

Li, W., Yang, K., Yin, S., Yang, X., Xu, Y., Lupoi, R., 2018. Solid-state additive manufacturing and repairing by cold spraying: A review. J. Mater. Sci. Technol. 34, 440–457. https://doi.org/10.1016/j.jmst.2017.09.015

Liu, D., Lippold, J.C., Li, J.I.A., Rohklin, S.R., Vollbrecht, J., Grylls, R., 2014. Laser engineered net shape (LENS) technology for the repair of Ni-base superalloy turbine components. Metall. Mater. Trans. A Phys. Metall. Mater. Sci. 45, 4454–4469.

https://doi.org/10.1007/s11661-014-2397-8

Liu, Q., Shi, S., Walker, K., Choi, Y.R., Brandt, M., 2017. Repair and Manufacturing of Military Aircraft Components by Additive Manufacturing Technology. 17th Australian International Aerospace Congress: AIAC 2017At: Melbourne, Australia.

Liu, Z., Jiang, Q., Ning, F., Kim, H., Cong, W., Xu, C., Zhang, H.C., 2018. Investigation of energy requirements and environmental performance for additive manufacturing processes. Sustain. 10. https://doi.org/10.3390/su10103606

Liu, Z.C., Jiang, Q.H., Zhang, H.C., 2013. LCA-based comparative evaluation of newly manufactured and remanufactured diesel engine. Re-Engineering Manuf. Sustain. - Proc. 20th CIRP Int. Conf. Life Cycle Eng. 663–667. https://doi.org/10.1007/978-981-4451-48-2_108

Machado, C.G., Despeisse, M., Winroth, M., Ribeiro da Silva, E.H.D., 2019. Additive manufacturing from the sustainability perspective: Proposal for a self-assessment tool. Procedia CIRP 81, 482–487. https://doi.org/10.1016/j.procir.2019.03.123

Mandil, G., Le, V.T., Paris, H., Suard, M., 2016. Building new entities from existing titanium part by electron beam melting: microstructures and mechanical properties. Int. J. Adv. Manuf. Technol. 85, 1835–1846. https://doi.org/10.1007/s00170-015-8049-3

Mani, M., Lyons, K.W., Gupta, S.K., 2014. Sustainability characterization for additive manufacturing. J. Res. Natl. Inst. Stand. Technol. 119, 419–428. https://doi.org/10.6028/jres.119.016

Martina, F., Ding, J., Williams, S., Caballero, A., Pardal, G., Quintino, L., 2019. Tandem metal inert gas process for high productivity wire arc additive manufacturing in stainless steel. Addit. Manuf. 25, 545–550. https://doi.org/10.1016/j.addma.2018.11.022.

Morrow, W.R., Qi, H., Kim, I., Mazumder, J., Skerlos, S.J., 2007. Environmental aspects of laser-based and conventional tool and die manufacturing. J. Clean. Prod. 15, 932-943. https://doi.org/10.1016/j.jclepro.2005.11.030.

Peng, S., Li, T., Wang, X., Dong, M., Liu, Z., Shi, J., Zhang, H., 2017. Toward a Sustainable Impeller Production: Environmental Impact Comparison of Different Impeller Manufacturing Methods. J. Ind. Ecol. 21, S216–S229. https://doi.org/10.1111/jiec.12628

Petrat, T., Graf, B., Gumenyuk, A., Rethmeier, M., 2016. Laser metal deposition as repair technology for a gas turbine burner made of inconel 718. Phys. Procedia 83, 761–768. https://doi.org/10.1016/j.phpro.2016.08.078

Pragana, J.P.M., Sampaio, R.F.V., Bragança, I.M.F., Silva, C.M.A., Martins, P.A.F., 2021. Hybrid metal additive manufacturing: A state–of–the-art review. Adv. Ind. Manuf. Eng. 2, https://doi.org/10.1016/j.aime.2021.100032

Priarone, P.C., Campatelli, G., Montevecchi, F., Venturini, G., Settineri, L., 2019. A modelling framework for comparing the environmental and economic performance of WAAM-based integrated manufacturing and machining. CIRP Ann.-Manuf. Techn. 68/1, 37-40. https://doi.org/10.1016/j.cirp.2019.04.005

Priarone, P.C., Pagone, E., Martina, F., Catalano, A.R., Settineri, L., 2020. Multi-criteria environmental and economic impact assessment of wire arc additive manufacturing. CIRP Ann.-Manuf. Techn. 69/1, 37-40. https://doi.org/10.1016/j.cirp.2020.04.010

Priarone, P.C., Robiglio, M., Settineri, L., 2018. On the concurrent optimization of environmental and economic targets for machining, J. Clean. Prod. 190, 630-644. https://doi.org/10.1016/j.jclepro.2018.04.163

Qi, H., Azer, M., Singh, P., 2010. Adaptive toolpath deposition method for laser net shape manufacturing and repair of turbine compressor airfoils. Int. J. Adv. Manuf. Technol. 48, 121–131. https://doi.org/10.1007/s00170-009-2265-7

Rahito, Wahab, D.A., Azman, A.H., 2019. Additive manufacturing for repair and restoration in remanufacturing: An overview from object design and systems perspectives. Processes 7. https://doi.org/10.3390/pr7110802

Rajeev, G.P., Kamaraj, M., Bakshi, S.R., 2017, Hardfacing of AISI H13 tool steel with Stellite 21 alloy using cold metal transfer welding process, Surf. Coatings Technol. 326/A, 63–71. https://doi.org/10.1016/j.surfcoat.2017.07.050.

Ramalho, A.L., Ferreira, J.A.M., Branco, C.A.G.M., 2011. Fatigue behaviour of T welded joints rehabilitated by tungsten inert gas and plasma dressing. Mater. Des. 32, 4705–4713. https://doi.org/10.1016/j.matdes.2011.06.051

Rosen, D.W., 2014. Research supporting principles for design for additive manufacturing: This paper provides a comprehensive review on current design principles and strategies for AM. Virtual Phys. Prototyp. 9, 225–232. https://doi.org/10.1080/17452759.2014.951530

Saboori, A., Aversa, A., Marchese, G., Biamino, S., Lombardi, M., Fino, P., 2019. Application of directed energy deposition-based additive manufacturing in repair. Appl. Sci. 9. https://doi.org/10.3390/app9163316

Sauerwein, M., Doubrovski, E., Balkenende, R., Bakker, C., 2019. Exploring the potential of additive manufacturing for product design in a circular economy. J. Clean. Prod. 226, 1138–1149. https://doi.org/10.1016/j.jclepro.2019.04.108

Scheel, C., Aguiñaga, E., Bello, B., 2020. Decoupling economic development from the consumption of finite resources using circular economy. A model for developing countries. Sustain. 12, 1–21. https://doi.org/10.3390/su12041291

Segers, R., 2008. Three options to calculate the percentage renewable energy: An example for a EU policy debate. Energy Policy. 2008;36:3243-3248. https://doi.org/10.1016/j.enpol.2008.05.014

Selvi, S., Vishvaksenan, A., Rajasekar, E., 2018. Cold metal transfer (CMT) technology - An overview. Def. Technol. 14, 28–44. https://doi.org/10.1016/j.dt.2017.08.002

Srinivas, M., Babu, B.S., 2017. A Critical Review on Recent Research Methodologies in Additive Manufacturing. Mater. Today Proc. 4, 9049–9059. https://doi.org/10.1016/j.matpr.2017.07.258

Sutherland, J.W., Adler, D.P., Haapala, K.R., Kumar, V., 2008. A comparison of manufacturing and remanufacturing energy intensities with application to diesel engine production. CIRP Ann.-Manuf. Technol. 57, 5–8. https://doi.org/10.1016/j.cirp.2008.03.004

Voestalpine Böhler Edelstahl GmbH & Co KG, 2018. Hot work tool steel, BW015 EN. Available at: www.voestalpine.com/bohler-edelstahl. Lastly accessed on February 3rd, 2021.

Walachowicz, F., Bernsdorf, I., Papenfuss, U., Zeller, C., Graichen, A., Navrotsky, V., Rajvanshi, N., Kiener, C., 2017. Comparative

Energy, Resource and Recycling Lifecycle Analysis of the Industrial Repair Process of Gas Turbine Burners Using Conventional Machining and Additive Manufacturing. J. Ind. Ecol. 21, S203–S215. https://doi.org/10.1111/jiec.12637

Wang, C., Suder, W., Ding, J., Williams, S., 2021. Wire based plasma arc and laser hybrid additive manufacture of Ti-6Al-4V. J. Mater. Process. Technol. 293, , ISSN 0924-0136, 117080. https://doi.org/10.1016/j.jmatprotec.2021.117080.

Wang, S., Gu, H., Wang, W., Li, C., Ren, L., Wang, Z., Zhai, Y., Ma, P., 2019. Study on Microstructural and Mechanical Properties of an Al–Cu–Sn Alloy Wall Deposited by Double-Wire Arc Additive Manufacturing Process. Materials 13, 73. https://doi.org/10.3390/ma13010073

Weinert, K., Inasaki, I., Sutherland, J.W., Wakabayashi, T., 2004. Dry Machining and Minimum Quantity Lubrication. CIRP Ann.-Manuf. Techn. 53/2, 511-537. https://doi.org/10.1016/S0007-8506(07)60027-4

Widener, C.A., Carter, M.J., Ozdemir, O.C., Hrabe, R.H., Hoiland, B., Stamey, T.E., Champagne, V.K., Eden, T.J., 2016. Application of High-Pressure Cold Spray for an Internal Bore Repair of a Navy Valve Actuator. J. Therm. Spray Technol. 25, 193–201. https://doi.org/10.1007/s11666-015-0366-4

Williams, S.W., Martina, F., Addison, A.C., Ding, J., Pardal, G., Colegrove, P., 2016. Wire + Arc Additive Manufacturing. Mater. Sci. Technol. 32, 641–647. https://doi.org/10.1179/1743284715Y.0000000073.

Wilson, J.M., Piya, C., Shin, Y.C., Zhao, F., Ramani, K., 2014. Remanufacturing of turbine blades by laser direct deposition with its energy and environmental impact analysis. J. Clean. Prod. 80, 170–178. https://doi.org/10.1016/j.jclepro.2014.05.084

Wits, W.W., García, J.R.R., Becker, J.M.J., 2016. How Additive Manufacturing Enables more Sustainable End-user Maintenance, Repair and Overhaul (MRO) Strategies. Procedia CIRP 40, 693–698. https://doi.org/10.1016/j.procir.2016.01.156

Wu, H.Q., Shi, Y., Xia, Q., Zhu, W.D., 2014. Effectiveness of the policy of circular economy in China: A DEA-based analysis for the period of 11th five-year-plan. Resour. Conserv. Recycl. 83, 163–175. https://doi.org/10.1016/j.resconrec.2013.10.003

Yin, S., Cavaliere, P., Aldwell, B., Jenkins, R., Liao, H., Li, W., Lupoi, R., 2018. Cold spray additive manufacturing and repair: Fundamentals and applications. Addit. Manuf. 21, 628–650. https://doi.org/10.1016/j.addma.2018.04.017

Yushchenko, K.A., Savchenko, V.S., Chervyakova, L. V., David, S.A., Vitek, J.M., 2004. Study of weldability and development of the technology for repair of high-Nickel alloy components.

Zhang, X., Li, W., Cui, W., Liou, F., 2018. Modeling of worn surface geometry for engine blade repair using Laser-aided Direct Metal Deposition process. Manuf. Lett. 15, 1–4. https://doi.org/10.1016/j.mfglet.2017.11.001

Zhang, X., Zhang, M., Zhang, H., Jiang, Z., Liu, C., Cai, W., 2020. A review on energy, environment and economic assessment in remanufacturing based on life cycle assessment method. J. Clean. Prod. 255, 120160. https://doi.org/10.1016/j.jclepro.2020.120160

Zheng, Y., Liu, J., Ahmad, R., 2020. A cost-driven process planning method for hybrid additive–subtractive remanufacturing. J. Manuf. Syst. 55, 248–263. https://doi.org/10.1016/j.jmsy.2020.03.006

Zhu, Y., Schwam, D., Wallace, J.F., Birceanu, S., 2004. Evaluation of soldering, washout and thermal fatigue resistance of advanced metal materials for aluminum die-casting dies. Mater. Sci. Eng. A 379, 420–431. https://doi.org/10.1016/j.msea.2004.03.020